Human θ Oscillations Related to Sensorimotor Integration and Spatial Learning

Jeremy B. Caplan,[1] **Joseph R. Madsen,**[2,3] **Andreas Schulze-Bonhage,**[4] **Richard Aschenbrenner-Scheibe,**[4] **Ehren L. Newman,**[1] **and Michael J. Kahana**[1,2]

[1]Volen Center for Complex Systems, Brandeis University, Waltham, Massachusetts 02454, [2]Department of Neurosurgery, Children's Hospital, Boston, Massachusetts 02115, [3]Department of Surgery, Harvard Medical School, Boston, Massachusetts 02115, and [4]Neurozentrum, Universität Freiburg, 79106 Freiburg, Germany

θ oscillations in the rat hippocampus have been implicated in sensorimotor integration (Bland, 1986), especially during exploratory and wayfinding behavior. We propose that human cortical θ activity coordinates sensory information with a motor plan to guide wayfinding behavior to known goal locations. To test this hypothesis, we analyzed invasive recordings from epileptic patients while they performed a spatially immersive, virtual taxi driver task. Consistent with this hypothesis, we found θ oscillations during both exploratory search and goal-seeking behavior and, in particular, during virtual movement, when sensory information and motor planning were both in flux, compared with periods of self-initiated stillness. θ oscillations had different topographic and spectral characteristics during searching than during goal-seeking, suggesting that different cortical networks exhibit θ depending on which cognitive functions are driving behavior (spatial learning during exploration vs orienting to a learned representation during goal-seeking). In contrast, oscillations in the β band appeared to be related to simple motor planning, likely a variant of the Rolandic μ rhythm. These findings suggest that human cortical θ oscillations act to coordinate sensory and motor brain activity in various brain regions to facilitate exploratory learning and navigational planning.

Key words: θ oscillations; intracranial electroencephalography; spatial navigation; spatial memory; sensorimotor integration; wayfinding

Introduction

Researchers have linked the prominent 3–12 Hz oscillations in rodent field recordings to conditioning (Seager et al., 2002), memory (Givens, 1996), path planning (O'Keefe and Recce, 1993), moving (Vanderwolf, 1969), orienting (Gavrilov et al., 1995), and exploration (Komisaruk, 1970; Macrides, 1975). Bland and Oddie proposed the sensorimotor integration hypothesis (i.e., that θ oscillations act to coordinate activity in various brain regions to update motor plans on the basis of sensory input) (Bland, 1986; Bland and Oddie, 2001).

We investigated the function of θ oscillations in the human brain. Note that traditionally in humans, the θ band is defined as 4–8 Hz (Niedermeyer, 1999). We conservatively define human θ as 4–8 Hz activity, consistent with both the human and rodent conventions. Recording intracranial electroencephalogram (iEEG) from human epileptic patients, bypassing the filtering of the skull (Sperling, 1997), we could record θ oscillations visible in the unfiltered signal (Kahana et al., 1999; Caplan et al., 2001). These θ oscillations appeared while participants learned to navigate virtual T-junction mazes, and their presence covaried with maze difficulty, suggesting that human θ oscillations play a role in spatial learning. Other evidence suggests that human cortical θ is present during active virtual movement (for review, see Kahana

et al., 2001). de Araújo et al. (2002) recorded magnetoencephalography (MEG) while healthy participants navigated virtual environments. They found greater θ power while participants were moving than during three control conditions. They did not manipulate spatial learning. Here, we link these two sets of findings by manipulating both virtual movement and the type of wayfinding within the same task and test the hypothesis that human θ oscillations are the physiological substrate for sensorimotor integration during exploration and seeking known locations using a learned representation.

We developed a task, "Yellow Cab," that encourages participants to find efficient paths from arbitrary locations. Participants were required to alternately search for passengers placed at random, unknown locations ("searching") and to seek learnable, fixed goal locations, occupied by stores ("goal-seeking").

If θ oscillations reflect sensorimotor integration, then we should see more θ during active virtual movement, when both sensory information and the motor program are in states of flux, than during voluntary stillness, even when those periods of stillness are part of the participant's intentional wayfinding behavior. The topography and frequencies of θ oscillations may depend on whether the participant is navigating to known locations in the environment (i.e., stores; goal-seeking) versus unknown locations (i.e., passengers; searching). Goal-seeking behavior should primarily recruit networks that are required for orienting to a learned representation relative to incoming sensory information, whereas searching behavior may in addition recruit networks involved in updating the spatial representation on the basis of new sensory information, given its exploratory function. We test these hypotheses by analyzing interleaved periods of movement

versus standing still and searching versus goal-seeking. We compare these findings with the same analyses in the β band (13–30 Hz), a characteristic component of the μ rhythm, related to motor planning (Jasper and Andrews, 1938; Niedermeyer, 1999; Klopp et al., 2001). Finally, we show that the θ oscillations we observe cannot simply reflect modulations of a resting posterior α rhythm.

Materials and Methods

Participants and recording

We recorded from 12 patients with medically resistant epilepsy (see Table 1 for demographics). Patients had subdural grids and depth electrodes implanted chronically to localize the seizure focus and to map functional regions to avoid in surgery. Recordings were acquired over 1–2 weeks. By participating in our studies, these patients incurred no additional medical or surgical risk, and informed consent was obtained from the patients and their guardians. The protocol was approved by the Institutional Review Boards at Children's Hospital (Boston, MA) and Neurozentrum, Universität Freiburg (Freiburg, Germany). Signal was sampled at 256 Hz, except for patient 6, who had a 512 Hz sampling rate. Bandpass filter was 0.3–70 Hz for patients at Children's Hospital (BioLogic) and 0.015–120 Hz for patients at Universität Freiburg (DeltaMed). The locations of the electrodes were determined from coregistered computed tomograms and magnetic resonance images by an indirect stereotactic technique (Talairach and Tournoux, 1988) or derived from stereotactic implantation (Freiburg). Electrodes overlying regions of known lesions or seizure onset zones or showing interictal spikes or sharp waves were excluded from analysis. Recordings at Children's Hospital were referred to a physically linked set of scalp electrodes. Recordings at Universität Freiburg were referred to an intracranial contact during acquisition and analyzed relative to a reference signal computed from an average of intracranial electrodes, excluding sites overlying seizure-onset zones or showing interictal artifacts.

Figure 1 shows the locations of all recording sites sampled, both included and excluded from analyses. Additionally, while participants 4, 6, and 8–11 had hippocampal as well as cortical recordings, the number of such sites was not large enough to enable us to make statements about oscillatory activity in the hippocampus. Therefore, we report findings from cortical recording sites only.

Task and procedure

Construction of virtual towns. The virtual towns were laid out on a 3 × 3 regular grid of roads, surrounded by an outer wall. The regularity of the layout facilitated automatic generation of the towns, randomizing the sets of stores and buildings and their locations in each town. Defining the width of a road as one unit (IU) in the virtual world, the size of the entire environment was 10 × 10 U. Of the 100 total square units, 36 square units consisted of nine equally sized blocks, each containing one structure (building or store). Blocks were separated from each other and

the outer wall by roads. Environments had six buildings and three stores (Fig. 2b).

Each building occupied ∼1 square unit centered within a block. Buildings could vary slightly in the area of their base and substantially in their height. Each building had a unique façade mapped onto all four walls and a lawn separating the building from the road (Fig. 2a). These nontarget structures provided a rich visual context for the virtual towns. The stores were of uniform shape and size, with a single storefront image mapped onto all four sides. Each store occupied a 0.7 × 0.7 × 0.35 U rectangular cube centered on each block. Unlike buildings, stores were not surrounded by a lawn but by paved roads that allowed participants to drive up to the storefronts.

The outer boundary of the environment had the image of a stone wall mapped along its length. No other heterogeneous visual information could be seen beyond this boundary.

Navigation. The virtual taxi allowed participants to navigate from a first-person point of view at an eye height of 0.1 U. The field of view was set to 56 × 44° in 640 × 480 mode. Participants used the four arrow keys on a standard keyboard to navigate. They could not make arcing turns; if more than one key was pressed, only the most recent key press would apply, and a key had to be released before it could be used again. The turning rate was 20°/sec such that it would take 18 sec to complete a full rotation. The walking speed was set to 1.17 U/sec. The view was refreshed every 30 msec. Pick up or delivery of passengers occurred when the participant came within 0.20 U of the passenger or the storefront, respectively.

During searching, a single would-be passenger was placed in the environment. On each delivery, the location of the next passenger was chosen randomly. When the passenger was picked up (by driving up to the passenger), a text screen appeared, instructing the participant to find a specific target store for a virtual fare. Participants pressed the "Enter" key; this was followed by a timed text screen reiterating the instructions to seek the target store. The text screen was displayed for 2 sec, after which participants were returned to the virtual town. The timed text screen was included to have a consistent, interleaved control task (reading control phase) to contrast with navigation. Because the forms of the text screens were constant throughout the task, the reading task may be more akin to a rest condition than to an actual reading task.

As soon as the passenger was delivered, another text screen was displayed, indicating success and instructing the participant to look for another passenger. Again, when participants pressed the Enter key, a 2 sec, timed text screen appeared, reiterating the instructions to search for a passenger, representing more reading control time. Participants were rewarded $50 virtual cash for each delivery and were docked $1 for every 10 sec spent moving, turning, or standing still, but there was a restriction that a maximum of $1 could be docked for any continuous period of standing still. Their earnings were continuously displayed in the top right corner of the screen. At the top left, a short description of their current

Table 1. Patient demographics

Patient	Age	Sex	Number of sites	Number excluded	Type	Resection	Hospital
1	15	Male	111	11	Subdural	Anterior frontal	B
2	18	Male	64	16	Subdural	Left temporal	B
3	14	Female	64	10	Subdural	Left amygdala/Left anterior hippocampus	B
4	15	Male	68	16	Both	Left temporal	B
5	15	Male	120	28	Subdural	Right frontal/temporal	B
6	42	Female	49	19	Both	Right temporal	F
7	28	Male	66	11	Both	Right inferior frontal/anterior temporal	F
8	33	Male	81	38	Both	Right posterior temporal/occipital	F
9	32	Female	60	23	Both	Left temporal/occipital	F
10	22	Male	27	19	Both	Right hippocampus	F
11	29	Male	34	22	Both	Right frontal	F
12	25	Male	78	33	Both	None[a]	F

Number of sites, Total number of cortical electrode contacts. Number excluded, Total number of recording sites excluded from analyses because of epilepsy-related pathology. Type, Type of electrodes placed; Subdural, subdural grids and strips; Both, both subdural and depth electrodes; B, Children's Hospital (Boston); F, Neurozentrum (Freiburg).

[a]Participant 12 had no resection, but seizure onset and interictal activity were seen broadly, centered around the right Sylvian fissure.
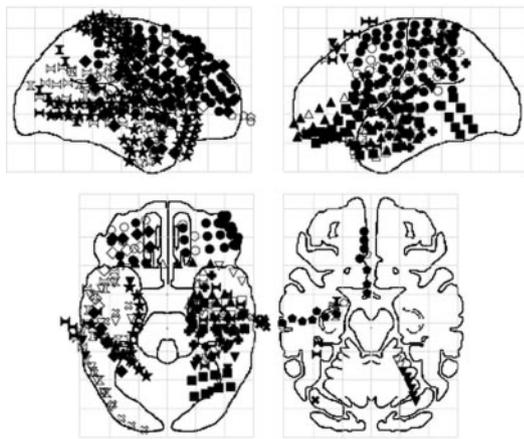
Figure 1. Locations of recordings sites across all 12 participants. These topographic maps show electrode locations on four views of a standard brain. Top left, Right lateral view. Top right, Left lateral view. Bottom left, Inferior view. Bottom right, Mid-axial/hippocampal view. Different shapes denote locations in different participants. Unfilled sites were excluded from our analyses; filled sites were included (see Materials and Methods).

goal was shown (e.g., "Find a passenger" or "Find the Java Zone"). This prevented participants from forgetting their current goal.

Procedure. Participants navigated in two distinct virtual towns. Before beginning the test environments, participants completed two different practice tasks. In the first task, participants delivered four passengers, one to each of four stores, in an open-field, practice environment. This practice environment was a 3 × 3 grid with four stores, one in each corner block. These stores were not used in the main task. The other blocks were covered with grass, which restricted movement to the paved areas without obstructing the participants' view. Navigating this practice environment familiarized participants with the controls of the taxi and with the method for picking up and delivering passengers.

In the second practice task, participants viewed the images of all six storefronts that would be encountered later in both towns. Below each image, the name of the store was displayed; these names were later used by passengers to indicate where they wanted to go. Participants looked at each picture and read its name aloud. The list was presented once in a random order and read at a self-paced rate. Then, the list was presented 10 times, each time in a new random order, at 2 sec per storefront and a 1 sec interstimulus interval. This practice task was designed to familiarize participants with the appearance of the stores before entering the towns. This task was repeated, with a new random presentation order, before navigating each environment.

Two towns were generated automatically for each participant, randomizing the sets of stores and buildings used, and their locations. To complete each environment, participants delivered 21 passengers, seven to each of the three stores. Before each test environment, participants repeated the second practice task (viewing and naming store fronts), but only performed the practice environment once, at the beginning of testing. Participants performed 21 deliveries in the first town, 21 deliveries in the second town, and, finally, were returned to the first town for 21 new randomized deliveries.

We recorded time-stamps for all key presses and stimulus presentation times, allowing us to recreate the sequence of events within the testing session.

Measuring learning
Learning was assessed by computing excess path length as a function of number of deliveries within a novel town. Excess path length was defined as the traveled path length minus the actual distance from start to finish, where the actual distance is approximated as the city-block distance ($\Delta X + \Delta Y$), and should decrease as participants find more efficient routes to goal locations.

Detecting oscillatory episodes
We used the oscillatory episode detection technique developed in previous work (Caplan et al., 2001). This method enables us to identify epochs of iEEG signal that exhibit high-power rhythmic activity at a particular frequency, lasting a few cycles, while excluding the estimated noise spectrum. An oscillatory episode at a particular frequency, f^* is defined as an epoch longer than a duration threshold, D_T (in number of cycles), during which power at frequency f^* exceeded a power threshold, P_T. The two threshold parameters were chosen as follows: (1) We wavelet transformed the raw traces [Morlet wavelet, window = six cycles (Grossmann and Morlet, 1985)] at 24 logarithmically spaced frequencies in the range of 1–54 Hz. This gave us wavelet power as a function of time at each frequency of interest. (2) We selected P_T separately for each frequency at each recording site. We assumed that the background spectrum was "colored noise" with the form $Af^{-\alpha}$. We estimated this background spectrum by fitting the observed spectrum for each electrode by computing a linear regression in log–log units. Because the wavelet power values are expected to be distributed like $\chi^2(2)$ (Percival and Walden, 1993), the estimated background power at frequency f^* would be the mean of that $\chi^2(2)$ distribution. We extrapolated to the 95th percentile of the fit distribution, and this was used as the threshold, $P_T(f^*)$ function, excluding ~95% of the estimated background signal. (3) D_T at frequency f^* was set to three cycles (i.e., $3\frac{1}{f^*}$) to eliminate artifacts and physiological signatures that were nonrhythmic. Both threshold values (95th percentile power threshold and three cycle duration threshold) were equal to those

a

b
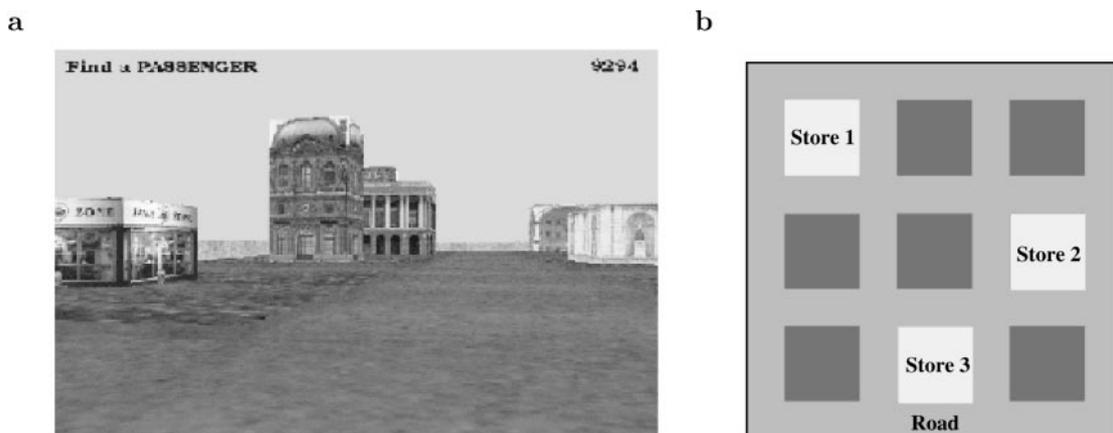
Figure 2. *a,* Sample screen shot from a first-person perspective. Participants viewed the environment in color. The road is textured gray, and grass is textured green, elevated from the road with a curb. A store (the "Java Zone") is visible on the left, and other (non-store) buildings are also visible. The stone-textured wall that surrounds the town is visible in the distance. The participant's goal is indicated in the top left corner, and the score is indicated in the top right corner. *b,* A blueprint of a sample environment layout (never seen by the participants). Note that there are three store blocks (light squares) and six building blocks (dark, unlabeled squares). The dark outline denotes the city wall.

used in previous work, in which we also found the qualitative nature of our results to be relatively insensitive to the precise choice of thresholds (Caplan et al., 2001). Finally, $P_{\text{episode}}(f)$, or percentage of time in episodes, was defined as the total amount of a time segment during which episodes occurred at frequency f divided by the total time in the segment of interest.

In subsequent analyses, we considered the 2–45 Hz range, excluding the frequencies at the ends of the spectrum. This was done to keep clear of the bandpass filtering of the amplifiers at the low-frequency end and to avoid contamination by the line noise artifact at the high end (60 Hz for Boston recordings; 50 Hz for Freiburg recordings).

To determine whether the sets of electrodes/frequencies in two analyses were similar or different, we correlated z-transformed test statistics (z-transformed Mann–Whitney U or t values) across electrodes and frequencies showing at least one effect to a liberal significance criterion. The significance criterion was selected to fix the type I error level across participants and to yield enough data to compute a reliable correlation. Therefore, the p value threshold was set to give a type I error of 0.5 comparison. If the correlation is significantly positive, this indicates that the two effects show the same topographic/spectral characteristics. If the correlation is significantly negative, this indicates that the two effects are anticorrelated or are significant at distinct sites and frequencies. If the correlation is nonsignificant, then we fail to reject the hypothesis that the two effects are independent.

Mapping the α rhythm
To induce resting posterior α activity, a computer-driven program played the recorded instructions to the participants to close their eyes for 5 sec and then open them for 5 sec, alternately for five repetitions.

Power at each frequency was computed using the same set of wavelets used in the task analyses. At each frequency, the sets of power values during eyes-closed periods and eyes-open periods were log-transformed and then compared using a two-tailed t test, accounting for the reduced degrees of freedom because of overlapping wavelets (Plett, 2000). Oscillatory episode detection was not used because that would yield only 5 $P_{\text{episode}}(f)$ values for each condition, too weak to perform a reasonable t test.

Results
Oscillations related to virtual movement
We asked whether any sites exhibited significantly heightened levels of θ oscillations during navigation (moving forward, turning left, and turning right) relative to the reading control phase ($p < 0.00001$; two-tailed Mann–Whitney U test). The total time analyzed during reading, moving while searching, and moving while goal-seeking was 535 ± 23, 2072 ± 101, and 1060 ± 76 sec, respectively (mean ± SEM across participants). The average time spent continuously in these three types of behavior was 2.00 ± 0.00, 2.02 ± 1.16, and 1.92 ± 0.15 sec, respectively. Indeed, 276 of the 584 sites had significant increases in $P_{\text{episode}}(f)$ in at least one sampled frequency within the θ band during searching. During goal-seeking, 338 sites exhibited movement-related θ. In contrast, far fewer showed the reverse effect (21 sites for searching vs reading; 19 sites for goal-seeking vs reading). This confirmed that θ oscillations were more prevalent during virtual movement than during a non-navigation control. However, these oscillations could have been related to being in the virtual town, or to virtual movement in particular, as predicted by the sensorimotor integration hypothesis.

To answer this question, we examined whether oscillations were more prevalent while the participant was moving in the virtual town relative to remaining "stationary." Periods of stillness, like periods of virtual movement, were under the participant's voluntary control. The total time analyzed during stillness while searching and goal-seeking was 277 ± 82 and 187 ± 55 sec, respectively (mean ± SEM). Mean time spent continuously stationary during searching and goal-seeking was 0.74 ± 0.08 and

0.87 ± 0.10 sec, respectively. Figure 3a shows a sample raw trace suggesting that θ oscillations are related to virtual movement. The average wavelet power spectrum (Fig. 3b) at this example site does not show an obvious peak in the θ band but does show differences between epochs of moving versus stillness that would be consistent with movement-related θ. When we apply the oscillatory episode detection algorithm and plot the percentage of time occupied by oscillatory episodes, $P_{\text{episode}}(f)$ as a function of behavior (Fig. 3c), the effect is much more apparent. The colored noise spectrum $[P(f) = Af^{-\alpha}]$, in which lower frequencies tend to have higher amplitudes than higher frequencies, has been accounted for, putting all frequencies on an equal footing. In addition to removing the bias across frequency, clear peaks can now be seen in the θ band (4–8 Hz) and β band (13–30 Hz). This suggests that the power spectrum was sensitive to signal other than contiguous runs of heightened power at a given frequency (e.g., nonoscillatory evoked potentials, spikes, and sharp waves, etc.). By removing a large portion of this nonoscillatory signal, one can analyze the oscillations more directly. Third, the $P_{\text{episode}}(f)$ plots show a clear difference between moving and stillness at this site. We next tested for this pattern at all recording sites.

We computed $P_{\text{episode}}(f)$ for each searching and goal-seeking path (from starting point to destination) across all continuous epochs of a particular type of behavior[a] (moving forward, turning left, turning right, or standing still), including only epochs of duration 0.5–30 sec, and compared the $P_{\text{episode}}(f)$ for movement versus standing still.

Many recording sites showed more θ oscillations related to virtual movement, during both searching (Fig. 4a; 278 sites) and goal-seeking (Fig. 4b; 87 sites) phases (two-tailed Mann–Whitney U test; $p < 0.0001$). The effect is widespread, including bilaterally in the peri-Rolandic region and the temporal lobes. In the case of goal-seeking, the effect is asymmetric, with more movement-related θ appearing in the right hemisphere, and notably less movement-related θ in dorsal regions. The movement-related θ effect in both searching and goal-seeking is strikingly unidirectional, with only one site showing more θ oscillations during standing still.

In addition to this effect being present in the θ band, it also showed significance at other frequencies, especially in the β band. Figure 5 shows the locations of sites showing movement-related β oscillations during searching (a; 290 sites) and goal-seeking (b; 123 sites), as well as the $P_{\text{episode}}(f)$ plot for an example electrode showing the effect in the β band (c). Movement-related β oscillations are found in widespread regions, but the effect is strongest in the peri-Rolandic region, supporting the notion that this signal related to the Rolandic motor μ rhythm (Jasper and Andrews, 1938; Niedermeyer, 1999; Klopp et al., 2001). Its presence at ventral sites, however, suggests that movement-related β activity may not be exclusively related to Rolandic μ rhythm.

Figure 6 shows the same for the γ band (searching, 54 sites; goal-seeking, 20 sites). The γ activity dominates neither the average spectrum nor the $P_{\text{episode}}(f)$ plots. Although the overall percentage of task time occupied by γ oscillations is small, these scarce oscillations nonetheless are significantly modulated by movement versus standing still (Fig. 6), which is reminiscent of the low levels of γ activity found during virtual maze navigation

---

[a] We initially analyzed oscillatory activity as a function of three distinct types of movement separately (moving forward, turning left, and turning right) against standing still. We performed these analyses both during searching and during goal-seeking. The sets of electrodes/frequencies showing movement-related oscillations were highly consistent across the three types of behavior. Therefore, for all analyses of movement, we collapse across moving forward, turning left, and turning right.

that nonetheless correlated significantly with a measure of degree of learning [Caplan et al. (2001), their Fig. 12]. Movement-related γ appeared primarily in the peri-Rolandic region. This may be a higher-frequency component of the Rolandic μ rhythm (Jasper and Andrews, 1938; Niedermeyer, 1999). However, its presence at ventral temporal and frontal sites suggests that γ oscillations could be involved in the memory-related aspects of the task, perhaps in activating object representations (Tallon-Baudry et al., 1996, 1999; Rodriguez et al., 1999; Howard et al., 2003). At all frequencies, it was rare for a site to show more oscillations during standing still than during virtual movement.

Comparing movement-related oscillations in searching and goal-seeking

The previous analyses revealed movement-related θ oscillation, supporting the sensorimotor integration hypothesis. A more complete analysis of the data revealed movement-related oscillations at a broad range of frequencies, including fast (>30 Hz) γ oscillations. Do these effects found during searching and goal-seeking reflect the same underlying phenomenon or distinct oscillating networks? Although the effect is stronger during searching, as evidenced by the greater number of sites showing the effect, it is still possible that oscillations at those frequencies and sites that correlated with movement during searching were generally the same as those that correlated with movement during goal-seeking, but with slightly different significance values.

First, we tested whether searching and goal-seeking represented different modes of learning. We tested whether the 12 participants could find shorter paths with increasing experience, reducing their excess path length (see Materials and Methods).
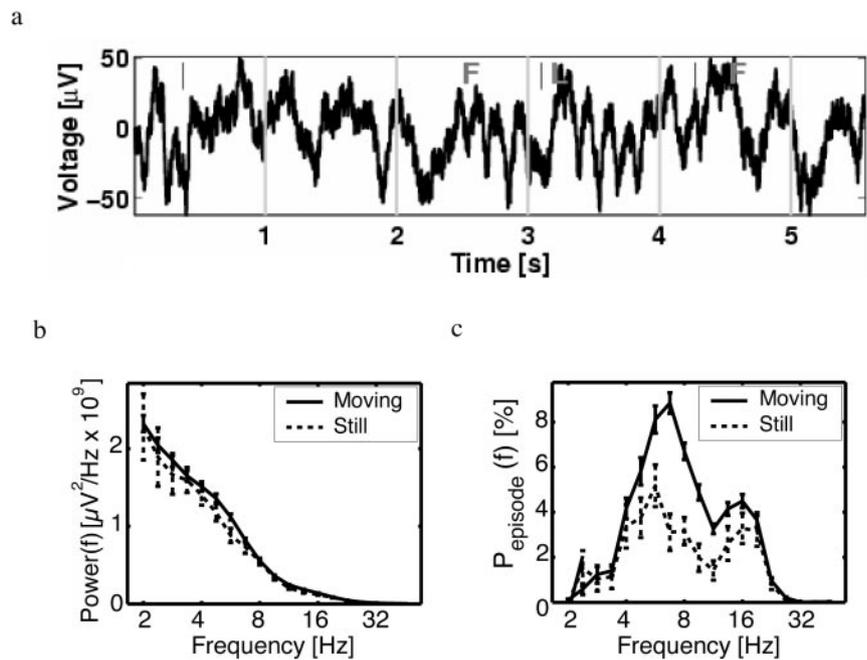
Figure 3. *a*, A sample intracranial EEG trace. Letters indicate the participant's keystrokes (F, up arrow; L, left arrow; |, released a key). *b*, Wavelet power spectrum averaged across searching paths while virtually moving (solid plot) or standing still (dashed plot). *c*, $P_{episode}(f)$ for searching paths while moving and standing still. Error bars denote SEM. All three plots are taken from participant 2, left inferior temporal gyrus [Talairach coordinates (left–right, anterior–posterior, inferior–superior) = −22, 40, −16 mm].

During goal-seeking, excess path length decreased significantly from the first set of three deliveries to the last nine deliveries within town B and the first session in town A ($t_{(11)} = 4.51$; $p < 0.001$), indicating that participants learned more efficient paths with experience in the town. In contrast, during searching, participants' excess path length did not change significantly from the first three searches to that last nine ($t_{(11)} = -0.41$; NS). This pattern did not change when we used Euclidean distance instead of city-block distance as the measure of actual distance (goal-seeking: $t_{(11)} = 4.66$, $p < 0.001$; searching: $t_{(11)} = -0.42$; NS). This suggests that our participants learned a spatial representation of the layouts of the towns and were able to use this infor-
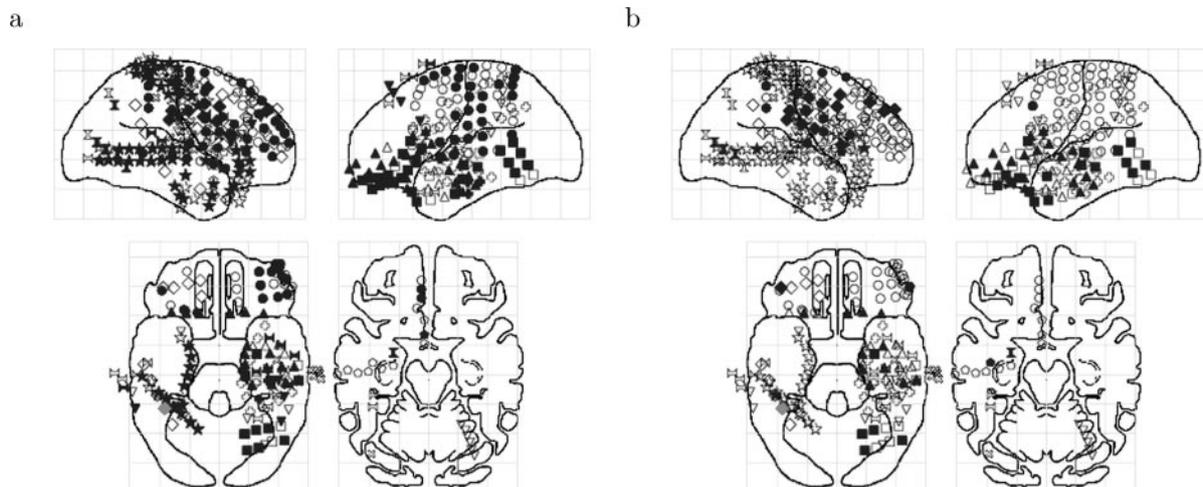
Figure 4. Movement-related θ oscillations. Dark-filled shapes denote sites showing more θ (4–8 Hz) during movement than when standing still (two-tailed Mann–Whitney *U* test; $p < 0.0001$) while searching (*a*) or while goal-seeking (*b*). Light-filled shapes showed the opposite pattern. Unfilled shapes denote sites included in the analyses that failed to reach significance. Estimated type I error rate = 0.29 sites.
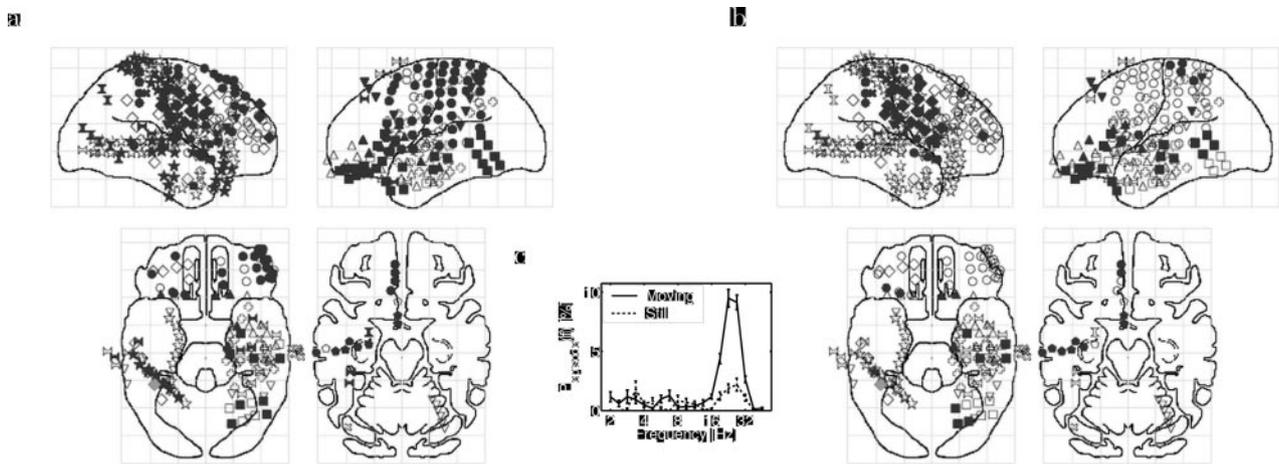
Figure 5. Movement-related β oscillations during searching (a) and goal-seeking (b). Dark-filled shapes denote sites showing more oscillations in the 13–30 Hz band during movement than when standing still (two-tailed Mann–Whitney U test; $p < 0.0001$). Light-filled shapes denote sites showing the opposite pattern. Unfilled shapes denote sites that did not show a significant effect. Estimated type I error rate = 0.29 sites. c, $P_{episode}(f)$ as a function of behavior during goal-seeking for an example site showing the effect [participant 6, Talairach coordinates (left–right, anterior–posterior, inferior–superior) = 52, −21, 52 mm]. Error bars denote SEM.

mation to find more efficient paths in goal-seeking but not in searching. Do these different types of wayfinding recruit different patterns of oscillations?

It is important to distinguish two hypotheses. The first hypothesis is that these oscillations are simply involved in virtual movement or key pressing. According to this hypothesis, the effect sizes should covary significantly positively across brain regions and frequencies between the searching and goal-seeking. The second hypothesis is that these oscillations are involved in spatial learning during exploration on the one hand (primarily during searching) and navigational planning on the other (primarily during goal-seeking). Thus, different sites and frequencies should be implicated in searching versus goal-seeking. In this case, the effect sizes should be independent or even anticorrelated between the searching and goal-seeking behavior.

We hypothesized that θ oscillations should be modulated by type of search, if they are involved in both spatial learning and navigational planning. For comparison, we hypothesized that oscillations in the β band are involved in simple motor planning of

the participants' key presses (Niedermeyer, 1999; Klopp et al., 2001). In this case, although the overall amount of motor planning may vary between searching and goal-seeking, we expect that the topographic and spectral characteristics should be the same, supporting the first hypothesis in the β band.

Visually comparing topography of movement-related θ in searching (Fig. 4a) and in goal-seeking (Fig. 4b) suggests that the two patterns differ substantially, especially in the peri-Rolandic region. We wanted to test for this difference quantitatively. Caplan et al. (2000) demonstrated that when analyzing significant thresholded data, a thresholding artifact could produce apparent differences in the patterns. They found that with a conservative significance threshold, a standard χ^2 test found the patterns of θ oscillations to be significantly different between study and test trials of a maze navigation task, but when thresholding more liberally, the patterns overlapped considerably. A conservative threshold reveals only the very most significant values, so which specific statistical comparisons pass a conservative threshold may be primarily determined by noise. To avoid such a
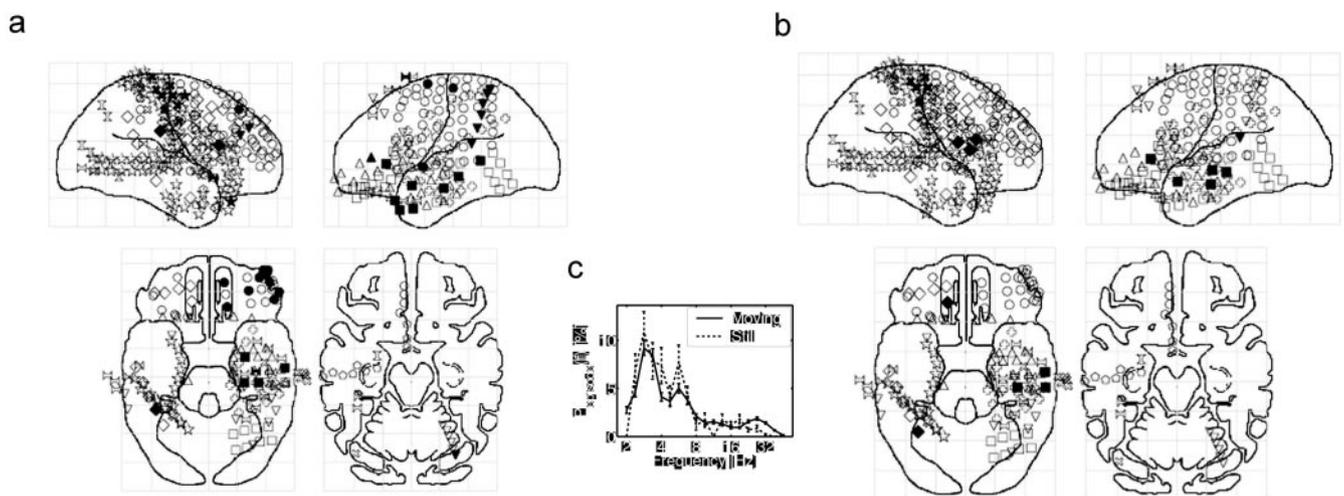
Figure 6. Movement-related γ oscillations during searching (a) and goal-seeking (b). Dark-filled shapes denote sites showing more oscillations in the 31–45 Hz band during movement than when standing still (two-tailed Mann–Whitney U test; $p < 0.0001$). Light-filled shapes denote sites showing the opposite pattern. Unfilled shapes denote sites that did not show a significant effect. Estimated type I error rate = 0.18 sites. c, $P_{episode}(f)$ as a function of behavior during searching for an example site showing the effect [participant 1, Talairach coordinates (left–right, anterior–posterior, inferior–superior) = −38.2, 52.9, −20.3 mm]. Error bars denote SEM.

Table 2. Correlation between movement-related oscillations during searching and goal-seeking in the θ and β bands

Participant	θ band	β band
1	−0.28 (267)***	0.31 (295)***
2	0.02 (199)	0.21 (206)**
3	0.18 (228)**	0.61 (64)***
4	−0.10 (39)	
5	0.24 (251)***	0.39 (191)***
6		0.78 (71)***
7	0.21 (113)*	0.41 (138)***
8	0.13 (90)	0.05 (124)
9	0.44 (90)***	0.77 (100)***
10	0.30 (36)	0.48 (31)**
11	0.04 (50)	0.59 (62)***
12	0.04 (171)	0.16 (171)*
Composite	0.07 (1559)**	0.38 (1474)***

Degrees of freedom are shown in parentheses. Each correlation was computed on the z-transformed test statistics across all recording sites and sampled frequencies in the θ band (4–8 Hz) or β band (13–30 Hz), given that at least one effect exceeded a significance threshold (see Materials and Methods). Missing data reflect insufficient statistical power to compute a reliable correlation (df, <10). The final row (Composite) shows correlations when combining data from all participants.

*p < 0.05; **p < 0.01; ***p < 0.001.

thresholding artifact, we noted that if the patterns are the same but experience some noise, then the statistical tests will be highly correlated across recording sites and frequencies; if the test for movement-related θ at a given frequency and electrode is strong during searching, we predict that it should also be strong during goal-seeking (at that same frequency and electrode). If the patterns are distinct, then knowing the strength of the effect at an electrode/frequency during searching should give no information about the significance during goal-seeking. In this case of independence, the correlation between the two patterns should be nonsignificant.

Table 2 shows the correlation values that test these hypotheses. As predicted, the set of sites/frequencies showing movement-related β oscillations during searching was highly similar to the set of sites/frequencies showing the effect in goal-seeking, for 10 of the 12 participants. Collapsing across all participants confirmed this result; the correlation is positive and highly significant: $r_{(1428)} = 0.39$; $p < 0.0001$.

However, in the θ band, we obtained mixed results. For participant 1, the two effects were anticorrelated. Because the movement-related θ was predominantly unidirectional for both searching and goal-seeking, this finding indicates that movement-related θ oscillations appeared at distinct sites/frequencies in searching rather than in goal-seeking. For participants 3, 5, 7, and 9, the effects covaried significantly in the positive direction, suggesting that the same sites/frequencies were showing movement-related oscillations during searching as during goal-seeking. For participants 2, 4, 8, 11, and 12 the effects failed to show a significant correlation, despite having substantial data, suggesting that for these participants, the effects were independent. Participant 6 did not have enough data to compute a reliable correlation. This variability could be partly attributable to differences in brain region sampling and partly caused by differences in the participants' strategies. Collapsing across all sites from all participants, the correlation in the θ band is quite small: $r_{(1504)} = 0.07$; $p < 0.01$. This suggests that at least a good portion of human cortical θ oscillations during virtual movement are not simply related to movement per se but may be present during specific aspects of search/seeking behavior, depending on brain region and frequency.

Although the topographic/spectral pattern characterizing
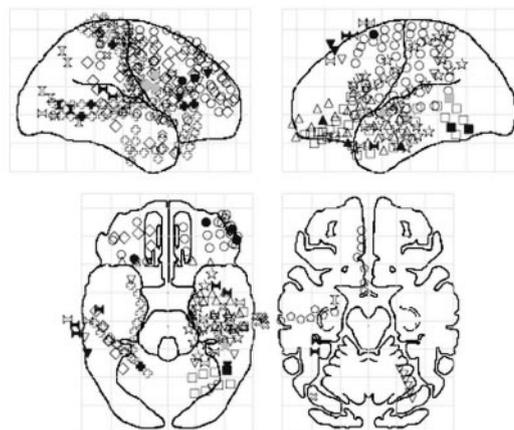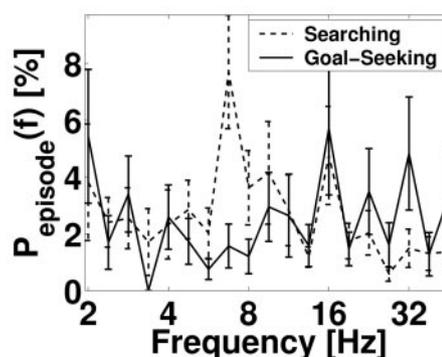
Figure 7. Type of search modulates oscillatory activity. a, Given that a site showed movement-related θ oscillations (4–8 Hz) during both searching and goal-seeking ($p < 0.1$), dark-filled shapes denote sites that showed higher levels of θ during searching than during goal-seeking ($p < 0.01$); light-filled shapes denote sites that showed the reverse effect. Estimated type I error rate = 12 sites. b, $P_{episode}(f)$ plot for searching (dashed plot) and goal-seeking (solid plot) for a site that showed this effect [participant 5, right fusiform gyrus, Talairach coordinates (left–right, anterior–posterior, inferior–superior) = 20, −52, −8 mm].

movement-related θ during searching is distinct from the pattern obtained during goal-seeking, some sites do show both effects within the θ band. We asked whether oscillations at these sites were more prevalent during searching or goal-seeking. If θ oscillations are related to learning during exploratory behavior, then we would expect θ more of the time during searching; if θ is related to retrieving information from a learned spatial representation or planning paths to known locations, then we would expect θ more of the time during goal-seeking.

We confined this analysis to sites showing movement-related oscillations at a given frequency during both searching and goal-seeking to a liberal significance criterion ($p = 0.1$); 443 sites met this initial criterion in at least one sampled θ frequency. We then tested whether sites showed significant differences in $P_{episode}(f)$ between searching and goal-seeking during epochs of virtual movement ($p < 0.01$). Figure 7 shows that a small subset of sites that showed movement-related θ (4–8 Hz) in both searching and goal-seeking showed a significant difference in $P_{episode}(f)$ between the two types of search. Thirty-eight sites showed more θ during searching than goal-seeking; six showed the reverse effect. However, of the 443 sites showing movement-related θ in both types of search, 268 failed to show a significant difference in levels of θ oscillations between searching and goal-seeking even

a

b
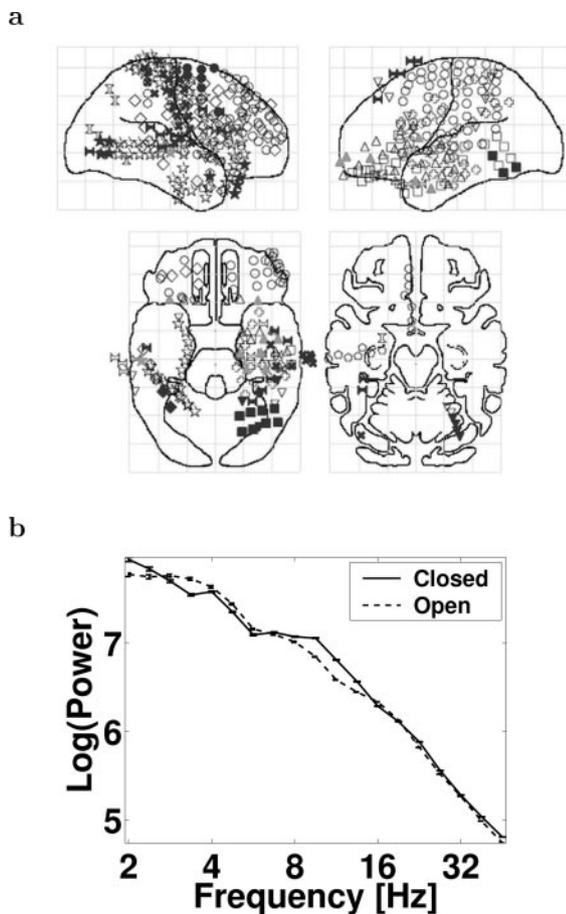
Figure 8. Resting posterior α rhythm. *a,* Sites that exhibit more α oscillations (8–12 Hz band) during eyes-closed periods (dark-filled sites) or during eyes-open periods (light-filled sites; two-tailed *t* test; *p* < 0.001). Estimated type I error rate = 0.12 sites. *b,* Example of a site showing this effect [participant 2, left medial temporal gyrus, Talairach coordinates (left–right, anterior–posterior, inferior–superior) = −62, −45, −2 mm]. Note a trend toward the opposite effect in the θ band, as commonly found in scalp recordings (Klimesch et al., 1993). Error bars denote SEM, with degrees of freedom corrected for the autocorrelation of the continuous wavelet transform. Power was used as the dependent measure instead of $P_{episode}(f)$, because there would have been too few observations to perform a statistically robust comparison.

when we used a very liberal significance criterion (*p* = 0.1). In summary, movement-related θ oscillations are either only found in searching or goal-seeking or tend to show comparable levels of θ during each type of search. However, when a difference is found, there tends to be more θ during searching than during goal-seeking.

Ruling out posterior resting α

To determine whether our findings could have resulted from modulations of the resting posterior α rhythm (Berger, 1929; Niedermeyer, 1999), we separately mapped the α rhythm (see Materials and Methods). The dark-filled sites in Figure 8 showed the resting α rhythm pattern (more oscillations during eyes-closed periods than eyes-open periods; *p* < 0.001). Many of these are in the posterior regions, also consistent with resting posterior α. Other sites show the opposite pattern (light-filled sites). These tend to be more anterior and ventral, consistent with the classic scalp-recorded α pattern.

In relation to our task analyses, first note the bipolar nature of the results. α shows primarily one effect in posterior sites and primarily the opposite effect elsewhere. If movement-related θ was a modulation of resting posterior α, it should also show this

bipolar pattern. In all comparisons, however, the task dependency was almost exclusively in one direction (either positive or negative).

Next, participants 1, 3, and 11 had no sites showing significantly more α oscillations during eyes-closed periods than eyes-open periods. This is likely attributable to the fact that we were not recording from regions that generate resting posterior α. For these participants, it is implausible that we are mistaking modulations in resting posterior α for movement-related θ.

For the remaining nine participants, we followed up by correlating the sets of sites and frequencies (within a more inclusive, 6–13 Hz band; the results do not change when using a narrower, 8–12 Hz band) in the α analysis with the pattern obtained in the task analyses. Here, sites were included in the analysis if they showed the movement-related oscillations and more oscillations during eyes-closed periods than during eyes-open periods. None of the nine participants showed a significant positive correlation (*p* < 0.05) between the α pattern and movement-related θ oscillations during searching or goal-seeking (Fig. 4), with the exception of participant 10, who showed a significant positive correlation between movement-related oscillations during searching with the pattern of resting posterior α ($r_{(38)}$ = 0.48; *p* < 0.005). Therefore, we can safely rule out α as an alternate account of the bulk of our task-dependent θ findings.

Discussion

Virtual navigation induced cortical θ activity. θ oscillations appeared more of the time during virtual movement than during interleaved periods of voluntary stillness, consistent with the MEG findings of de Araújo et al. (2002). These effects were found during two types of wayfinding: exploratory searching, in which the target locations were unknown, and goal-seeking to fixed targets, allowing participants to make use of learned knowledge about the layout of the town. The topographic and spectral characteristics of movement-related θ, however, differed between searching and goal-seeking, especially in peri-Rolandic regions. This suggests that the network of brain regions exhibiting θ oscillations depends on which regions are involved in a particular kind of behavior and, in particular, which regions are required for sensorimotor integration. The pattern of movement-related θ found during goal-seeking may primarily act to coordinate brain regions during wayfinding. The pattern found during searching may be primarily involved in learning that spatial layout during exploratory behavior. Movement-related β and γ oscillations were also observed. The β activity, which had topographic and spectral characteristics during searching that were very similar to those seen during goal-seeking behavior, may be involved in motor planning and might be related to the Rolandic μ rhythm (Jasper and Andrews, 1938; Niedermeyer, 1999; Klopp et al., 2001). This buttresses the finding that oscillations in the θ band are modulated by searching versus goal-seeking.

The most well characterized human EEG rhythm is the resting posterior α rhythm, typically 8–12 Hz (Berger, 1929; Niedermeyer, 1999); this rhythm is routinely observed in the raw, scalp-recorded EEG during light sleep and resting wakefulness. It originates in the posterior portion of the neocortex and tends to be anticorrelated with θ power (Klimesch, 1999). Could our findings be modulations of the resting posterior α rhythm, especially given that our patient population may have abnormal α frequencies? Our task-related oscillations might reflect the degree of drowsiness or inattentiveness (Gevins et al., 1997) rather than cognitive function. We ruled out this possibility by directly comparing our virtual navigation findings with the empirically ob-

tained pattern of α and found that it had different topographic and spectral properties than movement-related θ.

Cortical θ in rodents

Unlike most rodent studies that have focused on hippocampal θ, we recorded task-dependent θ in the human neocortex. Physiologically, cortical θ in rodents may be closely related to hippocampal θ. Lukatch and MacIver (1997) analyzed carbachol-induced θ in cortical slices, finding that these oscillations exhibited similar responses to various drugs, including bicuculline, atropine, CNQX, and APV, as has been shown in hippocampal slices. Bland and Colom (1993) reviewed the studies of hippocampal, septal, cingulate, and entorhinal θ oscillations and suggested that the limbic cortex contains multiple synchronizing systems. Manns et al. (2002) provided evidence that different populations of medial septal cells control θ in different cortical regions. These dynamics could provide a means for lower brain regions to selectively induce θ in patterns of hippocampus and various cortical regions, depending on task demands. This selective control could in turn produce coherence among θ oscillations in multiple cortical regions (Manns et al., 2002). However, there is no *a priori* reason to assume that navigational strategies are the same in the human as in the rodent brain.

Human cortical θ may represent a local physiological state conducive to local learning for synapses in the vicinity of the field oscillation. Alternatively, cortical θ may act to synchronize activity between the hippocampus and cortical regions or between pairs of cortical regions. In the following sections, we consider the evidence for each function of cortical θ in turn, and then discuss how they may be brought together in our task.

Virtual versus real navigation

We chose virtual navigation rather than real navigation for practical considerations: its ease of use in a hospital setting, control over the visual properties of the task, and obtaining precise timing of the participants' responses. Virtual reality has been used extensively in recent years to study human spatial behavior (Klatzky et al., 1998; Redlick et al., 2001; Warren et al., 2001; Lambrey et al., 2002) (E. L. Newman, J. B. Caplan, M. P. Kirschen, R. Sekuler, and M. J. Kahana, unpublished observations) and physiology (Kahana et al., 1999; Burgess et al., 2002; de Araújo et al., 2002; Pine et al., 2002). The principal difference between real and virtual navigation is that in the latter, participants lack vestibular cues. Human participants can path integrate using visual cues alone (Redlick et al., 2001; Warren et al., 2001), and Witmer et al. (1996) found that participants could transfer route knowledge they learned in a virtual setting to its real-world equivalent. Thus, what is learned may be similar with or without vestibular input. Lambrey et al. (2002) found that when vestibular and visual input conflict, participants appear to learn both conflicting sets of information, favoring the visual source when visual cues are available and favoring the vestibular when blindfolded, highlighting the flexibility of navigation behavior. However, Klatzky et al. (1998) found that the participants made fewer turning errors when they walked along a path than when they experienced optic flow in a virtual setting. Thus, vestibular input certainly appears to enhance spatial updating.

The physiological place representation appears to be intact with or without vestibular input. Matsumura et al. (1999) found place cells in monkey hippocampus while monkeys were performing real or virtual movement. Furthermore, Dees et al. (2001) found comparable levels of rat hippocampal θ during navigation with or without vestibular cues. It is quite possible that, with vestibular input, human θ oscillations would show similar task dependencies in additional, vestibular sensory regions in the neocortex. Thus, the general function of θ oscillations may be preserved across sensory modalities, whereas the localization of this activity could vary with modality. A real-movement condition would be useful in future designs to address this question directly.

θ and coordinated activity of brain regions

One class of theories implicates θ oscillations in coordinating the activity of multiple brain regions. It has been proposed in two papers (Bland, 1986; Bland and Oddie, 2001) that rodent θ oscillations coordinate sensory and motor brain regions during types of behavior that require the animal to update its motor plan on the basis of incoming sensory information. This hypothesis would predict more θ during virtual movement than periods of stillness, as reported here and in a MEG study by de Araújo et al. (2002). It would also account for the finding of θ during wayfinding to known targets, as found during goal-seeking.

Other researchers have proposed that information is encoded in the phase within an oscillation (McLardy, 1959; Adey et al., 1962; Landfield, 1977; Jensen et al., 1996) (D. S. Rizzuto, J. R. Madsen, E. Bromfield, A. Schulze-Bonhage, D. Seelig, R. Aschenbrenner-Scheibe, and Kahana, unpublished observations). Jensen (2001) also demonstrated that θ oscillations could act like carrier waves for information transfer between any pair of regions, via synchronized oscillations at the same frequency. These approaches are all consistent with the notion that θ oscillations are critical for coordinating activity during wayfinding, as well as during exploratory (virtual) movement. Cortical sites exhibiting θ could be acting simultaneously, but not interacting, in which case θ might represent a specific kind of physiologically "active" state. Alternatively, sites exhibiting θ could be interacting with the hippocampus via oscillations at distinct, rather than the same, frequencies (for example, accessing a hippocampal "cognitive map") (O'Keefe and Nadel, 1978) or interacting with other cortical (or hippocampal) regions via oscillations at the same frequency (Bland and Oddie, 2001; Jensen, 2001).

θ and learning

In contrast to theories that implicate θ in coordinating activity in disparate brain regions, another class of theories implicates θ in local synaptic plasticity and learning at the behavioral level.

θ oscillations have been linked to the induction of long-term potentiation (LTP) and long-term depotentiation, and stimulation that mimics the θ rhythm is effective in inducing LTP (Larson and Lynch, 1986, 1989; Larson et al., 1986). Furthermore, the phase of the θ rhythm determines whether synapses will be potentiated or depotentiated (Pavlides et al., 1988; Huerta and Lisman, 1995; Hölscher et al., 1997; Orr et al., 2001). Manipulations that suppress θ oscillations tend to impair learning (Landfield et al., 1972; Landfield, 1977; Winson, 1978; Givens and Olton, 1990; Mizumori et al., 1990). Several drugs known to improve memory function in rats were shown to enhance θ amplitude (Kinney et al., 1999). Finally, both θ power and frequency show a systematic shift during the course of conditioning in the cat (Grastyán et al., 1959; Adey et al., 1960), and θ frequency is predictive of spatial learning rate in the rat (Berry and Thompson, 1978), suggesting that amplitude and frequency as well as phase are critical for learning.

More directly linking naturally occurring θ and learning, Seager et al. (2002) measured the rate of conditioning in rabbits while recording from their hippocampus. They presented condi-

tioning pairs when θ power was either high or low. Animals in the high-θ group took fewer trials to learn the response than their yoked controls, whereas those in the low-θ group required more trials than their controls. This suggests that naturally varying θ is critical for learning, perhaps because synaptic plasticity is modulated by the phase of naturally varying θ (Orr et al., 2001).

Our previous finding of increased θ during navigation of more complex mazes (Kahana et al., 1999; Caplan et al., 2001) and our present findings of increased θ during movement and searching are consistent with θ being involved in spatial learning.

Learning coordinated brain activity
One possibility is that θ may coordinate brain activity in different regions. In contrast, θ may be a physiological state underlying learning at the local network level. These two classes of theories may be linked. In particular, the type of learning that θ oscillations facilitate may necessarily involve learning coordinated interactions among different brain regions. For instance, Buzsáki (1996) proposed that learning is consolidated by transferring information from the hippocampus to the neocortex, mediated by cortical θ oscillations.

Bland and Oddie (2001) pointed out that the paradigms used to implicate θ in memory involved learning an association between a motor response and a sensory stimulus. Some models of human navigation propose that the learned representation is comprised of associations between local views (sensory information) and movements (motor planning) (Schölkopf and Mallot, 1995; Mallot et al., 1997). Thus, the models learn to do sensorimotor integration. The notion that θ accompanies learning of associations between sensory stimuli and motor behavior could account for previous findings of θ oscillations in the human cortex during virtual maze learning (Kahana et al., 1999; Caplan et al., 2001).

Conclusions
We propose that the patterns of cortical θ found during virtual taxi driving reflect two different, but related, functions. First, during goal-seeking, θ underlies updating motor plans in response to incoming sensory information during wayfinding. Second, during exploratory searching behavior, θ facilitates the encoding of coordinated activity in multiple brain regions and that this is the information that comprises the participant's cognitive map.

References
Adey WR, Dunlop CW, Hendrix CE (1960) Hippocampal slow waves: distribution and phase relationships in the course of approach learning. Arch Neurol 3:96/74–112/90.
Adey WR, Walter DO, Lindsley DF (1962) Subthalamic lesions: effects on learned behavior and correlated hippocampal and subcortical slow-wave activity. Arch Neurol 6:34–47.
Berger H (1929) Über das Elektroenkephalogramm des Menschen. Archiv für Psychiatrie und Nervenkrank 87:527–570.
Berry SD, Thompson RF (1978) Prediction of learning rate from the hippocampal electroencephalogram. Science 200:1298–1300.
Bland BH (1986) The physiology and pharmacology of hippocampal formation theta rhythms. Prog Neurobiol 26:1–54.
Bland BH, Colom LV (1993) Extrinsic and intrinsic properties underlying oscillation and synchrony in limbic cortex. Prog Neurobiol 41:157–208.
Bland BH, Oddie SD (2001) theta band oscillation and synchrony in the hippocampal formation and associated structures: the case for its role in sensorimotor integration. Behav Brain Res 127:119–136.
Burgess N, Maguire EA, O'Keefe J (2002) The human hippocampus and spatial and episodic memory. Neuron 35:625–641.
Buzsáki G (1996) The hippocampo-neocortical dialogue. Cereb Cortex 6:81–92.
Caplan JB, Kahana MJ, Sekuler R, Kirschen MP, Madsen JR (2000) Task dependence of human theta: the case for multiple cognitive functions. Neurocomputing 32–33:659–665.
Caplan JB, Kahana MJ, Raghavachari S, Madsen JR (2001) Distinct patterns of brain oscillations underlie two basic parameters of human maze learning. J Neurophysiol 86:368–380.
de Araújo DB, Baffa O, Wakai RT (2002) theta oscillations and human navigation: a magnetoencephalography study. J Cognit Neurosci 14:70–78.
Dees JA, Terrazas A, Bohne KM, Krause M, McNaughton BL, Barnes CA (2001) Presence of hippocampal theta during navigation without actual movement. Soc Neurosci Abstr 27:643.13.
Gavrilov VV, Wiener SI, Berthoz A (1995) Enhanced hippocampal theta EEG during whole body rotation in awake restrained rats. Neurosci Lett 197:239–241.
Gevins A, Smith ME, McEvoy L, Yu D (1997) High-resolution EEG mapping of cortical activation related to working memory: effects of task difficulty, type of processing, and practice. Cereb Cortex 7:374–385.
Givens B (1996) Stimulus-evoked resetting of the dentate theta rhythm: relation to working memory. NeuroReport 8:159–163.
Givens BS, Olton DS (1990) Cholinergic and GABAergic modulation of medial septal area: effect on working memory. Behav Neurosci 104:849–855.
Grastyán E, Lissák K, Madarász I, Donhoffer H (1959) Hippocampal electrical activity during the development of conditioned reflexes. Electroencephalogr Clin Neurophysiol 11:409–430.
Grossmann A, Morlet J (1985) . Decomposition of functions into wavelets of constant shape, and related transforms. In: Mathematics and physics, Vol 1 (Streit L, ed), pp 135–165. Singapore: World Scientific.
Hölscher C, Anwyl R, Rowan MJ (1997) Stimulation on the positive phase of hippocampal theta rhythm induces long-term potentiation that can be depotentiated by stimulation on the negative phase in area CA1 in vivo. J Neurosci 17:6470–6477.
Howard MW, Rizzuto DS, Caplan JB, Madsen JR, Lisman J, Aschenbrenner-Scheibe R, Schulze-Bonhage A, Kahana MJ (2003) Gamma oscillations correlate with working memory load in humans. Cereb Cortex, in press.
Huerta PT, Lisman JE (1995) Bidirectional synaptic plasticity induced by a single burst during cholinergic theta oscillation in CA1 in vitro. Neuron 15:1053–1063.
Jasper HH, Andrews HL (1938) Electro-encephalography. III. Normal differentiation of occipital and precentral regions in man. Arch Neurol Psychiatry 39:96–115.
Jensen O (2001) Information transfer between rhythmically coupled networks: reading the hippocampal phase code. Neural Comput 13:2743–2761.
Jensen O, Idiart MAP, Lisman JE (1996) Physiologically realistic formation of autoassociative memory in networks with theta/gamma oscillations: role of fast NMDA channels. Learn Mem 3:243–256.
Kahana MJ, Sekuler R, Caplan JB, Kirschen MP, Madsen JR (1999) Human theta oscillations exhibit task dependence during virtual maze navigation. Nature 399:781–784.
Kahana MJ, Seelig D, Madsen JR (2001) Theta returns. Curr Opin Neurobiol 11:739–744.
Kinney GG, Patino P, Mermet-Bouvier Y, Starrett JE, Gribkoff VK (1999) Cognition-enhancing drugs increased stimulated hippocampal theta rhythm amplitude in the urethane-anesthetized rat. J Pharmacol Exp Ther 29:99–106.
Klatzky RL, Loomis JM, Beall AC, Chance SS, Golledge RG (1998) Spatial updating of self-position and orientation during real, imagined, and virtual locomotion. Psychol Sci 9:293–298.
Klimesch W (1999) EEG α and theta oscillations reflect cognitive and memory performance: a review and analysis. Brain Res Brain Res Rev 29:169–195.
Klimesch W, Schimke H, Pfurtscheller G (1993) Alpha frequency, cognitive load and memory performance. Brain Topogr 5:241–251.
Klopp J, Marinkovic K, Clarke J, Chauvel P, Nenov V, Halgren E (2001) Timing and localization of movement-related spectral changes in the human peri-rolandic cortex: intracranial recordings. NeuroImage 14:391–405.
Komisaruk BR (1970) Synchrony between limbic system theta activity and rhythmical behavior in rats. J Comp Physiol Psychol 70:482–492.
Lambrey S, Viaud-Delmon I, Berthoz A (2002) Influence of a sensorimotor conflict on the memorization of a path traveled in virtual reality. Cognit Brain Res 14:177–186.

Landfield PW (1977) Different effects of posttrial driving or blocking of the theta rhythm on avoidance learning in rats. Physiol Behav 18:439–445.

Landfield PW, McGaugh JL, Tusa RJ (1972) theta rhythm: a temporal correlate of memory storage processes in the rat. Science 175:87–89.

Larson J, Lynch G (1986) Induction of synaptic potentiation in hippocampus by patterned stimulation involves two events. Science 232:985–988.

Larson J, Lynch G (1989) theta pattern stimulation and the induction of LTP: the sequence in which synapses are stimulated determines the degree to which they potentiate. Brain Res 489:49–58.

Larson J, Wong D, Lynch G (1986) Patterned stimulation at the theta frequency is optimal for the induction of hippocampal long-term potentiation. Brain Res 368:347–350.

Lukatch HS, MacIver MB (1997) Physiology, pharmacology, and topography of cholinergic neocortical oscillations *in vitro*. J Neurophysiol 77:2427–2445.

Macrides F (1975) Temporal relationships between hippocampal slow waves and exploratory sniffing in hamsters. Behav Biol 14:295–308.

Mallot HA, Franz M, Schölkopf B, Bülthoff HH (1997) The view-graph approach to visual navigation and spatial memory. Paper presented at Seventh International Conference on Artificial Neural Networks, Lausanne, Switzerland, October.

Manns ID, Alonso A, Jones BE (2002) Rhythmically discharging basal forebrain units comprise cholinergic, GABAergic and putative glutamatergic cells. J Neurophysiol 89:1057–1066.

Matsumura N, Nishijo H, Tamura R, Eifuku S, Endo S, Ono T (1999) Spatial- and task-dependent neuronal responses during real and virtual translocation in the monkey hippocampal formation. J Neurosci 19:2381–2393.

McLardy T (1959) Hippocampal formation of brain as detector-coder of temporal patterns of information. Perspect Biol Med 3:443–452.

Mizumori SJY, Perez GM, Alvarado MC, Barnes CA, McNaughton BL (1990) Reversible inactivation of the medial septum differentially affects two forms of learning in rats. Brain Res 528:12–20.

Niedermeyer E (1999) The normal EEG of the waking adult. In: Electroencephalography: basic principles, clinical applications, and related fields, Ed 4 (Niedermeyer E, Lopes da Silva F, eds), pp 149–173. Philadelphia: Lippincott Williams and Wilkins.

O'Keefe J, Nadel L (1978) The hippocampus as a cognitive map. New York: Oxford UP.

O'Keefe J, Recce ML (1993) Phase relationship between hippocampal place units and the EEG theta rhythm. Hippocampus 3:317–330.

Orr G, Rao G, Houston FP, McNaughton BL, Barnes CA (2001) Hippocampal synaptic plasticity is modulated by theta rhythm in the fascia dentata of adult and aged freely behaving rats. Hippocampus 11:647–654.

Pavlides C, Greenstein YJ, Grudman M, Winson J (1988) Long-term potentiation in the dentate gyrus is induced preferentially on the positive phase of theta-rhythm. Brain Res 439:383–387.

Percival DB, Walden AT (1993) Spectral analysis for physical applications: multitaper and conventional univariate techniques. Cambridge, UK: Cambridge UP.

Pine DS, Grun J, Maguire E, Burgess N, Zarahn E, Koda V, Fyer A, Szeszko PR, Bilder RM (2002) Neurodevelopmental aspects of spatial navigation: a virtual reality fMRI study. NeuroImage 15:396–406.

Plett MI (2000) Ultrasonic arterial vibrometry with wavelet based detection and estimation. PhD thesis, University of Washington.

Redlick FP, Jenkin M, Harris LR (2001) Humans can use optic flow to estimate distance of travel. Vision Res 41:213–219.

Rodriguez E, George N, Lachaux J-P, Martinerie J, Renault B, Varela FJ (1999) Perception's shadow: long-distance synchronization of human brain activity. Nature 4:430–433.

Schölkopf B, Mallot HA (1995) View-based cognitive mapping and path planning. Adaptive Behav 3:311–348.

Seager MA, Johnson LD, Chabot ES, Asaka Y, Berry SD (2002) Oscillatory brain states and learning: impact of hippocampal theta-contingent training. Proc Natl Acad Sci USA 99:1616–1620.

Sperling MR (1997) Clinical challenges in invasive monitoring in epilepsy surgery. Epilepsia 38:S6–S12.

Talairach J, Tournoux P (1988) Co-planar stereotaxic atlas of the human brain. Stuttgart, Germany: Verlag.

Tallon-Baudry C, Bertrand O, Delpuech C, Pernier J (1996) Stimulus specificity of phase-locked and non-phase-locked 40 Hz visual responses in human. J Neurosci 16:4240–4249.

Tallon-Baudry C, Kreiter A, Bertrand O (1999) Sustained and transient oscillatory responses in the gamma and beta bands in a visual short-term memory task in humans. Vis Neurosci 16:449–459.

Vanderwolf CH (1969) Hippocampal electrical activity and voluntary movement of the rat. Electroencephalogr Clin Neurophysiol 26:407–418.

Warren WH, Kay BA, Zosh WD, Duchon AP, Sahuc S (2001) Optic flow is used to control human walking. Nat Neurosci 4:213–216.

Winson J (1978) Loss of hippocampal theta rhythm results in spatial memory deficit in the rat. Science 201:160–163.

Witmer BG, Bailey JH, Knerr BW (1996) Virtual spaces and real world places: transfer of route knowledge. Int J Hum Comput Stud 45:413–428.